JOURNAL OF Applied Polymer SCIENCE

Analysis of Void Shape and Size in the Collector Plate and Polycaprolactone Molecular Weight on Electrospun Scaffold Pore Size

Jong Kyu Hong,[1] Guan Xu,[2] Daqing Piao,[2] Sundararajan V. Madihally[1]
[1]School of Chemical Engineering, Oklahoma State University, 423 Engineering North, Stillwater, Oklahoma 74078
[2]School of Electrical and Computer Engineering, Oklahoma State University, 202 Engineering South, Stillwater, Oklahoma 74078
Correspondence to: S. V. Madihally (E-mail: sundar.madihally@okstate.edu)

ABSTRACT: Many variations in the electrospinning process have emerged to control pore size needed in tissue scaffolds including introducing voids in the collector plate. However, the effect of different shapes and sizes of voids on fiber and pore sizes is not well understood. In this study, we evaluated the effect of void size and shapes in the collector plate on polycaprolactone (PCL) fiber size and pore size. First, we performed experiments using three different sizes of circular voids (0.9, 1.4, and 1.9 cm). Also, we evaluated the effect of triangular and rectangular voids. Further, changes in the electrical field within the voids were evaluated using computational fluid dynamic software COMSOL. Fibers using mixtures of PCL (high, medium, and low molecular weight) formed using void collector plate and performed degradation characteristics for 30 days in physiological conditions (37°C and 7.4 pH). These results showed that the size and the morphology of fibers are not affected by the geometrical patterns of the voids. However, fiber alignment is affected by the void shape due to favorable rearrangement in the electrical field. Fibers can be formed by mixing PCL of different molecular weight, and degradation of PCL fiber was accelerated by the mixture with low molecular weight. © 2012 Wiley Periodicals, Inc. J. Appl. Polym. Sci. 000: 000–000, 2012

KEYWORDS: biopolymers and renewable polymers; degradation; biomaterials; bioengineering; biomedical applications

Received 21 May 2012; accepted 7 July 2012; published online
DOI: 10.1002/app.38326

INTRODUCTION

While cells regenerate the tissue, the scaffold made of biodegradable polymers fades in the human body. The challenge is the design of scaffold to mimic natural extracellular matrix (ECM), which regulate cell behaviors such as cell migration, proliferation, and differentiation.[1] Electrospinning has been extensively studied for fabricating micro and nanosize fibers in tissue engineering due to the possibility of mimicking ECM characteristics. Because the intent of using scaffold is to guide the cells in forming structures with required shape and architecture, patterning the fibers during electrospinning has also been studied in relevance to cell colonization. Aligned fibers have been shown to promote organized regeneration of periodontal tissue,[2] myotubes,[3] primary and secondary neurons,[4] Schwann cells,[5] fibroblasts,[6] and endothelial cells.[7] Human skeletal muscle cells aligned along the fibers and formed better myotubes than randomly oriented fibers.[3] Fiber alignment also helps in developing anisotropy in the mechanical properties of the structures,[8] which may be necessary in certain tissues.

It is well understood that size of pores present between fibers (referred to as the pore size) influences cellular activity. The pore diameter must be controllable for cells to infiltrate into the scaffold and attach to the fibers below the surface. Also, scaffold pore size and shape are important to the alignment of cells and mechanical property of the tissue.[9] When electrospun fibers are used, the pore size between the fibers (less than 20 μm) is smaller than mammalian cells, restricting cells to grow on the top surface of the scaffold only. To fabricate scaffolds of electrospun fibers with aligned fibers and pore sizes required for cell infiltration, variation in collector plates with rectangular air gaps have been proposed.[10] Inclined collector plate with rectangular air gap is shown to align the fibers.[11] Others have used air gaps in the collector plate to produce scaffolds with larger pore size [12] and nerve guides.[13] Alternatively, air gaps can be introduced in the flat collector plate, which allows collection of fibers with increased pore sizes.[14] Formed fibrous structures allow cell colonization in three-dimensional form, gluing different layers of fibers. However, the effect of void size and shape on orientation and sizes of fibers is not well understood. Changes in the void space and shape could alter the electrical field, which influence the deposition of fibers.

Polycaprolactone (PCL) has been used to generate scaffolds for tissue regeneration due to biodegradability, nontoxicity, and

biocompatibility under physiological conditions.[15,16] Typically, high molecular weight PCL is used to generate electrospun fibers. Even though electrospun fibers made of high molecular weight PCL have various merits, the clinical usage is limited due to the long period of degradation *in vitro* and *in vivo* study (6 month–4 years).[17,18] Reduced molecular weight of PCL is necessary to improve the degradation rate. However, the electrospun fibers with low molecular weight of PCL are seldom fabricated due to processing difficulty such as low viscosity.

In this study, we questioned how the void size and shape effect the fiber distribution and orientation. Experiments were performed with different void shapes and sizes, and changes in fiber size and pore size were quantified. Simulations were performed to understand the changes in electrical field with different void shapes and sizes. Further, fibers were formed with mixed molecular weights (high, medium, and low) of PCL to overcome the limitation of PCL fiber with low molecular weight. First different ratios were evaluated and then, the effect of blending on the degradation of fibers was tested under the physiological conditions. These results show significant influence of void shape on fiber alignment without altering fiber size and possibility of forming PCL fibers using mixed molecular weight.

MATERIALS AND METHOD

Materials

PCLs (PCL80K, M_n = 80,000 and PCL10K, M_w = 14,000) and hexafluoro-2-propanol (HFP) were purchased from Sigma (St Louis, MO) and PCL45K (M_w =43,000–50,000) was obtained from Polysciences (Warrington, PA). Chloroform and methanol were purchased from Pharmco (Brookfield, CT). All materials were used without further purification.

Fabrication of Fiber with Different Void Sizes

Electrospinning apparatus consisted of a syringe pump (74900 series, Cole-Parmer Instrument Company, Vernon Hills, IL), BD 10 mL syringe (Luer-Lok Tip; Becton Dickinson and Company, Franklin Lakes, NJ), needle tip, high voltage power supply (ES30P-5W/DAM, Gamma High Voltage Research, Ormond Beach, FL), earth grounding, and various sizes and shapes of collector plate. Ten wt/v % was prepared by dissolving PCL in HFP and stirred for 24 h at room temperature. Flow rate, needle size, high voltage supply, and distance between the needle tip and the collector were 2 μL/h, 24 G, 12 kV, and 9 cm, respectively. The collector plate with 0.9, 1.4, or 1.9 cm diameter void and 1.2 cm deep were engraved in a wooden frame (3 $\times$ 10 $\times$ 2 cm^3), which was wrapped with aluminum foil.

Electrospinning with Different Void Shapes

Electrospinning setup described above was used to evaluate the effect of shape of the void with changes in collector. Flow rate, needle size, high voltage supply, and distance between the needle tip and the collector were 10 mL/h, 20 G, 10 kV, and 9 cm. Circular (1.5 cm diameter), triangular (the each side 1.5cm long), and rectangular (1 cm wide $\times$ 5 cm height) void shapes were engraved in wooden frames (3 cm height $\times$ 10cm length $\times$ 2 cm depth) to a depth of 1.2 cm. However, 22 wt/v % PCL was dissolved in a mixture of chloroform and methanol (9 to 1 ratio).

Effect of Different Molecular Weights of PCL

The fabrication conditions were similar to those described above except the polymer solution. Flow rate, needle size, high voltage supply, and distance between the needle tip and the collector were10 mL/h, 20 G, 10 kV, and 9 cm, respectively. The collector plate with a 1.9 cm circular void was used. The polymer solution with different concentration of PCL80K, 45K, and 10K ranging from 5.1 to 24% were dissolved in a mixture of chloroform and methanol (9 to 1 ratio) (Table I) and tested for fiber formation.

Degradation of PCL Fibers

Three fiber compositions with the same total polymer concentration but different mixing ratio of PCL80K/45K/10K (22 : 0 : 0, 11 : 11 : 0, or 9 : 9 : 4, respectively) were selected from Table 1. Fibers were formed under the same conditions described above and incubated in Krebs-Henseleit buffer solution (pH 7.4) at CO_2 incubator at 37°C for 30 days. The morphology of single fiber before and after the degradation was confirmed by using scanning electron microscope (SEM).

Microstructure Characterization

Samples were analyzed using JEOL 6360 (Jeol USA, Peabody, MA) SEM at an accelerated voltage of 9–30 kV similar to our previous publications.[19] In brief, samples were attached to an aluminum stub using a conductive graphite glue (Ted Pella, Redding, CA) and sputter coated with gold for 40 s before SEM analysis. Using the digital micrographs, fiber diameters, pore sizes, and shape factors of pores ($4\pi \times$ area/perimeter^2) were quantified using Sigma Scan Pro (SPSS Science, Chicago, IL). More than 50 points of fibers and pores were analyzed for each condition.

COMPUTATIONAL SIMULATION

To understand the changes in the electrical field due to the air gap in the collector plate, commercially available computational package COMSOL 3.5a Multiphysics (COMSOL, Burlington, MA) was used. In particular, the "Electrostatics" option available within the "Electromagnetics module" of COMSOL was used. Geometries were constructed according to the experimental setup for both the conventional and novel collector design. The distribution of the electric field and potential was simulated in a 14 $\times$ 10 $\times$ 3 cm^3 cubic volume. Next, the subdomain and boundary conditions were set in the Physics tab. The basic equation used in this simulation was Laplacian equation given by

$$\nabla^2 \phi = 0.$$

where ϕ is the electric potential field. It was assumed that the gap between the needle and collector frame was filled with air at 1 atm thereby the relative permittivity was set as 1 and the relative permittivity of the wood frame was set as 2. All surfaces covered by aluminum foil were set to zero potential (ground) and the needle surface was set at 20 kV, similar to the applied voltage in experimental conditions. The walls of the hole in the wood frame was set as continuous to electric field, and all the outer boundaries were set as zero charge because there is no actual dielectric interfaces at these boundaries.

Table I. PCL Fiber with Different Mixing Ratio of Molecular Weight 80 K, 45 K, and 10 K

Number of mixing components	Total concentration (w/v %)	PCL 80 K (w/v %)	45 K (w/v%)	10 K (w/v%)	Fiber
1	22	22			OK
1	20	20	-	-	OK
1	20	-	20	-	OK
1	20	-	-	20	DNW
2	22	11	11		OK
2	20	10	10	-	OK
2	20	10	-	10	DNW
2	20	-	10	10	DNW
3	20.1	6.7	6.7	6.7	DNW
2	18	9	9	-	OK
3	20	9	9	2	OK
3	22	9	9	4	OK
3	24	9	9	6	DNW
3	26	9	9	8	DNW
2	10	5	5	-	DNW
2	10	-	5	5	DNW
2	10	5	-	5	DNW
3	5.1	1.7	1.7	1.7	DNW
3	9.9	3.3	3.3	3.3	DNW
3	15	5	5	5	DNW

OK means the fiber was fabricated on the gap of the new collector plate under the fixed condition. For all the fibers, flow rate, needle size, high voltage supply, and distance between the needle tip and the collector were10 mL/h, 20 G, 10 kV, and 9 cm with the novel collector plate (diameter, 1.9 cm and depth 1.2 cm) in a wooden frame ($3 \times 10 \times 2$ cm^3) wrapped with aluminium foil. DNW means that the fiber was not collected under the above condition of the fibers.

RESULTS

Effect of Different Circular Void Sizes

Previously, we reported the effect of a circular void space of 1.4 cm in the collector plate on the micro and nanosize fibers of PCL relative to a conventional collector plate using a mixture of chloroform and methanol.[14] Quantification of fibers formed under the same conditions of solution and process parameters showed that circular void shape did not affect the fiber size and the shape of the pores between the fibers in the scaffolds. One could control the fiber sizes using appropriate solvents and distance of the collector plate similar to conventional settings. In this study, we extended that analysis to understand the effect of void sizes in the collector plate on the distribution of fibers formed at very slow rate using HFP as the solvent (Figure 1). The void size was increased from 0.9 cm via 1.4–1.9 cm [Figure 1(A–C)], and fibers were deposited for the same period of time using the same solution concentration and process parameters.

Analysis of digital micrograpahs showed that the fiber diameter and shape of the pores in structures [Figure 1(D–F)] did not change; however, the pore sizes increased. Unlike the distribution in the voids, the density of the fibers was high in the aluminum frame and they were deposited randomly on the aluminum frame [Figure 1(D–F)]. The fibers on the voids and on the aluminum frame were randomly oriented in the same pattern, suggesting that the fiber orientation was independent of the size of the circular void and the solvent. Likewise, the morphology of fibers was not affected by the void size in the collector plate.

Micrographs were further quantified for fiber diameters, shape factors, and sizes of pore between the fibers [Figure 1(G–I)]. The average fiber diameters were nearly 400 nm and the shape factors of the pores in structures was 0.50, independent of the circular void size. The primary effect of increased void size was the increase in the distance between the fibers; the average pore sizes increased from 14.71, 22.83, and 57.77 μm, with increased void size from 0.9, via 1.4 and 1.9 cm, respectively. Also, the distance between the fibers increased leading to increased void size because fewer layers of fibers deposited in the void of the new collector plate. Solution and process parameters of electrospinning mainly govern the size of the fibers.

Effect of Void Shape on the Fiber Characteristics

Next, we tested the effect of circular, triangular, and rectangular [(Figure 2(A–C)] void shapes on the pattern of deposited fibers in the collector plate. A mixture of chloroform and methanol was used similar to our previous publication.[14] These results showed that the distribution pattern depends on the void shape.

Applied Polymer SCIENCE

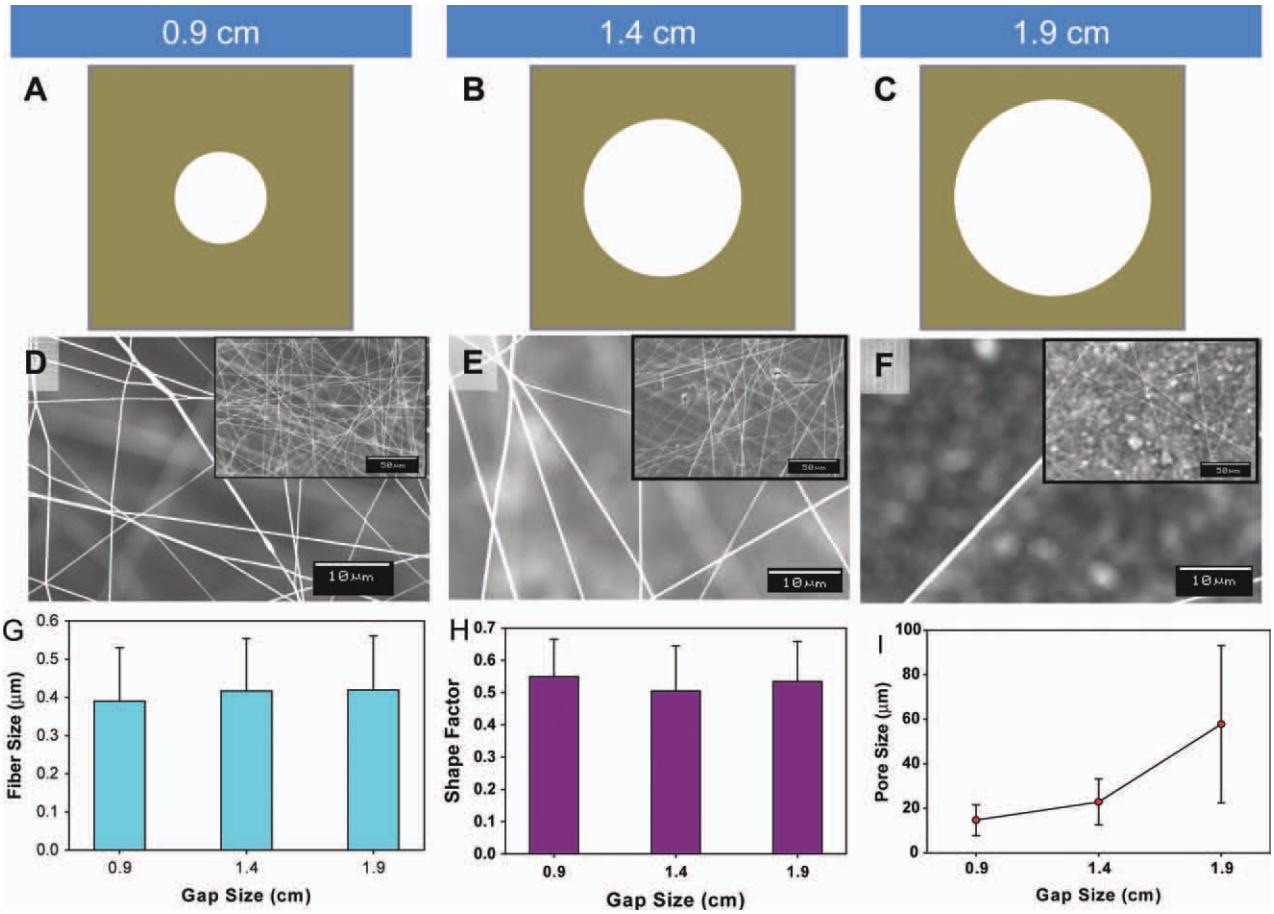

Figure 1. Schematics of the void size and polymeric structure of electrospun fibers. (A–C) The schematic of the void size in the collector plates and (D–F) scanning electron micrographs of electrospun nanofibers made of PCL in HFP increasing the void size from 0.9 via 1.4–1.9 cm. Inset in (D–F) are micrographs with low magnification showing pore size distribution. (G) Fiber diameters. (H) Shape factor. (I) Pore size. The error bars correspond to the standard deviation ($n = 50$). [Color figure can be viewed in the online issue, which is available at wileyonlinelibrary.com.]

As expected, the fibers were randomly deposited throughout the entire circular void of the collector plate [Figure 2(D,G)], despite changes in the solvent mixture. For the triangular voids, the fibers aligned perpendicular to the bisector at the edge of the vertices. However, the fibers at the middle of the void were randomly deposited [Figure 2(E,H)]. For the rectangular voids, the fibers aligned from one short side to the other side perpendicular to the long sides of the rectangle in large scale [Figure 2(F,I)]. Within the void, some fibers also showed random deposition. Evaluation of the patterns of the fibers in the aluminum frame showed high density of randomly deposited fibers in all the void shapes [Figure 2(D–F)]. The size and the morphology of fibers did not appear to be affected by the geometrical patterns of the void.

Effect of MW on Fiber Characteristics

The space distribution of fibers allows the charaterization of fibers without interference from adjacent fibers. For example, one could understand the degradation process or the stability of two polymers. Because PCL degradation rate is dependent on MW, we choose to evaluate the effect of making the scaffolds and the degradation process. Forming electrospun fibers using PCL10K alone was difficult due to the low viscosity of the solution; the lower molecular weight forms droplets at the needle tips. Fiber formation was also limited with different molecular weight mixing ratio from 9 : 9 : 0 to 9 : 9 : 4.

To understand the effect of different MW on fiber morhology in the voids, collected fibers were evaluated using scanning electron micrographs obtained from random regions. Quantification study revealed that the collector plate configuration does not influence the fiber size and the shape of the pores in the scaffold (Figure 3) for the same concentration of polymers at the same processing conditions. For example, when 20% PCL of 80 kDa was used, average fiber sizes on both collector plates were ~ 2 μm and both shape factors were ~ 0.50. These values are similar to our previous results, despite changes in polymer molecular weight.[14] Even when the concentration and mixing ratio of polymer solution was changed, no significant difference of fiber size and shape of the pore was obtained under the same processing conditions. These pore size values are similar to our previous results and are suitable for cell infiltration and cell colonization.[14]

To understand the effect of blending on degradation of the fibrous network, PCL80K fibers mixed with low molecular weight

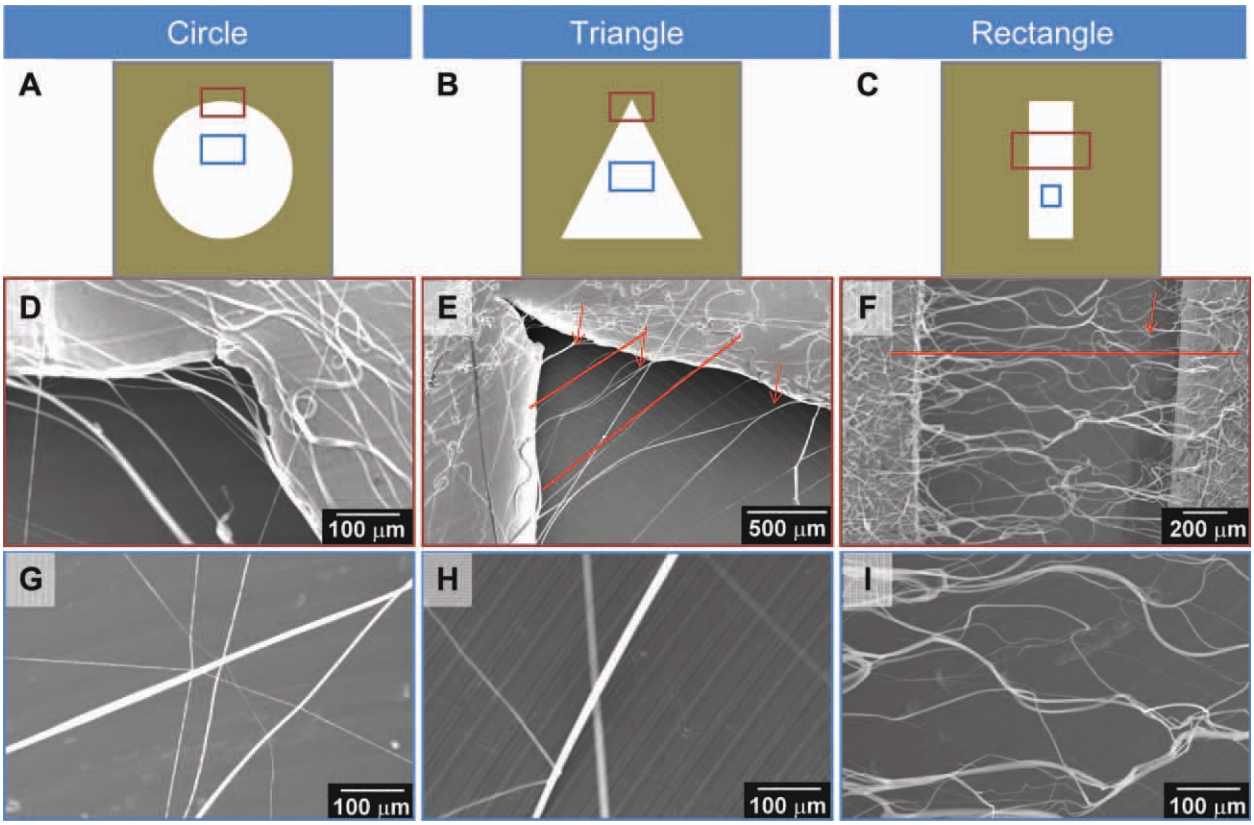

Figure 2. Schematics of the different shapes of the void in the collector plates and polymeric structure of electrospun fibers. The polymeric structure of the fibers with (A) circular, (B) triangular, and (C) rectangular shape of the void in the new collector plate. (D–I) Scanning electron micrographs of electrospun nanofibers made of PCL in a mixture of chloroform and methanol with different shapes of the void. [Color figure can be viewed in the online issue, which is available at wileyonlinelibrary.com.]

(PCL45K and PCL10K) were incubated in Krebs-Henseleit buffer solution (pH 7.4) at CO_2 incubator at 37°C for 30 days. The fibers made of PCL80K (22 : 0 : 0), PCL80K/45K (11 : 11 : 0), and PCL80K/45K/10K (9 : 9 : 4) were fabricated under the same processing conditions (Figure 4). The average fiber sizes were $\sim$ 2 μm in all cases (Figure 4(A–C)]. After 30 days of incubation, the surface morphology of the fibers was similar to those before the incubation in the majority of the fibers except in a few locations where fibers had tiny grooves and cracks on their surface [Figure 4(D–F)]. The degree of the surface damage increased in the fibers fabricated with PCL 80K/45K/10K compared to those made of PCL 80K or PCL 80K/45K. A few cracks existed on the surface of PCL 80K or PCL 80K/45K. However, the PCL80K/45K/10K fibers were cut. Thus, two parts of the fibers exist. These results demonstrate that the presence of 10 K PCL promotes disintegration of the fibers.

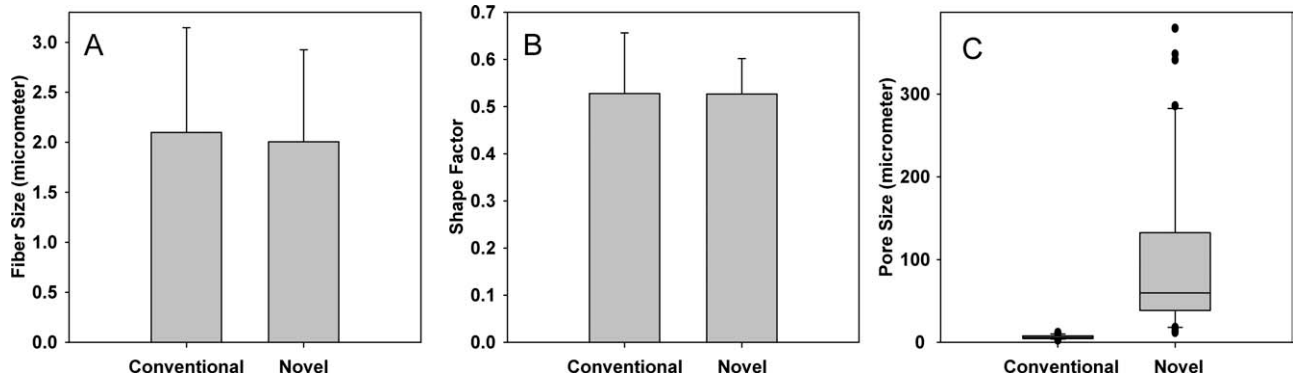

Figure 3. Effect of void space on PCL80K fiber characteristics. (A) Fiber diameters, the positive error bars correspond to the standard deviation (n = 50). (B) Shape factor, the positive error bars correspond to the standard deviation (n = 50). (C) Box plot showing the distribution of pore size with 10th, 25th, 50th, 75th, and 90th percentiles and the mean value (thick line within each box). Values that were outside 95th and 5th percentiles were treated as outliers.

Applied Polymer SCIENCE

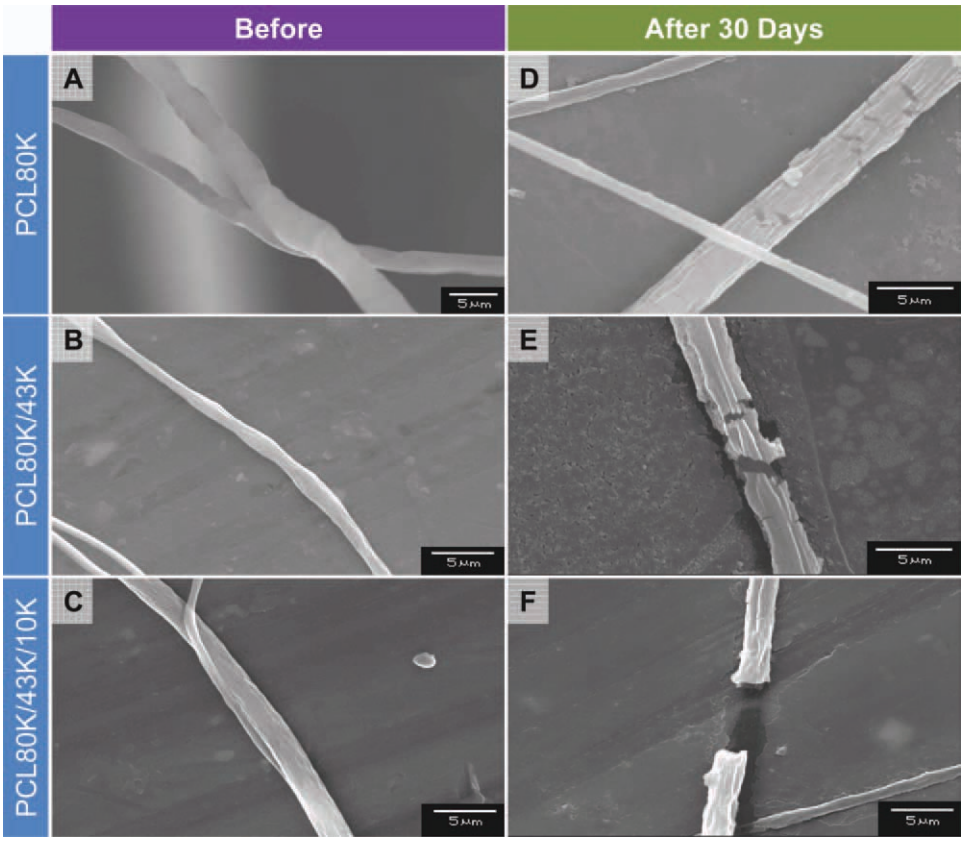

Figure 4. Effect of blending different PCL molecular weights on degradation of fibers. (A–C) The polymeric structure of fibers made of PCL80K, PCL80K/45K, and PCL80K/45K/10K after incubation under the physiological condition for 30 days.

Alterations in the Electrical Field

To understand the changes in the electrical field, equations were solved using COMSOL for different cases of voids in the collector plate. Obtained electric potential distributions and the isopotential surfaces were plotted. The conventional collector plate design [Figure 5(A)] produced planar isopotential surface and thus the cone-shaped polymer spray originating from the needle tip will evenly distribute on the collector surface. These results are similar to that reported in literature.[11] However, the isopotential surface collapses in the voids of the collector plate [Figure 5(B)]. Because the dragging force generated by the electric field will be perpendicular to the isopotential surfaces and the polymer fibers will be directed along the steepest potential descent direction, that is, to take the shorter path with respect to its initial launching direction, as is denoted by dashed lines (Figure 5). Thus, the majority of polymer fibers accumulate at

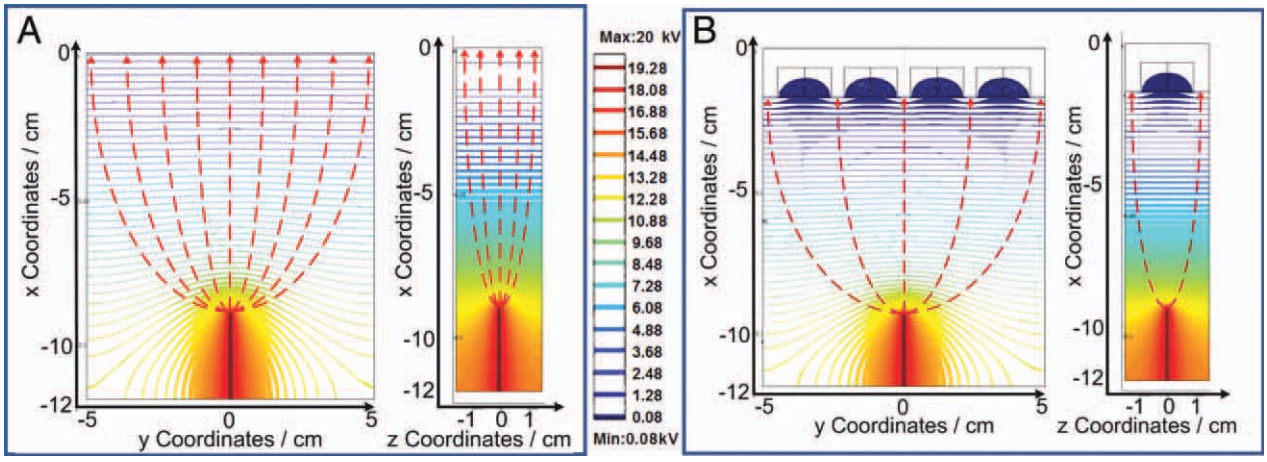

Figure 5. Effect of void space on the electrical field under 20 kV applied voltage. (A) Conventional collector plate. (B) Novel collector plate with four voids each of 14 mm size. [Color figure can be viewed in the online issue, which is available at wileyonlinelibrary.com.]

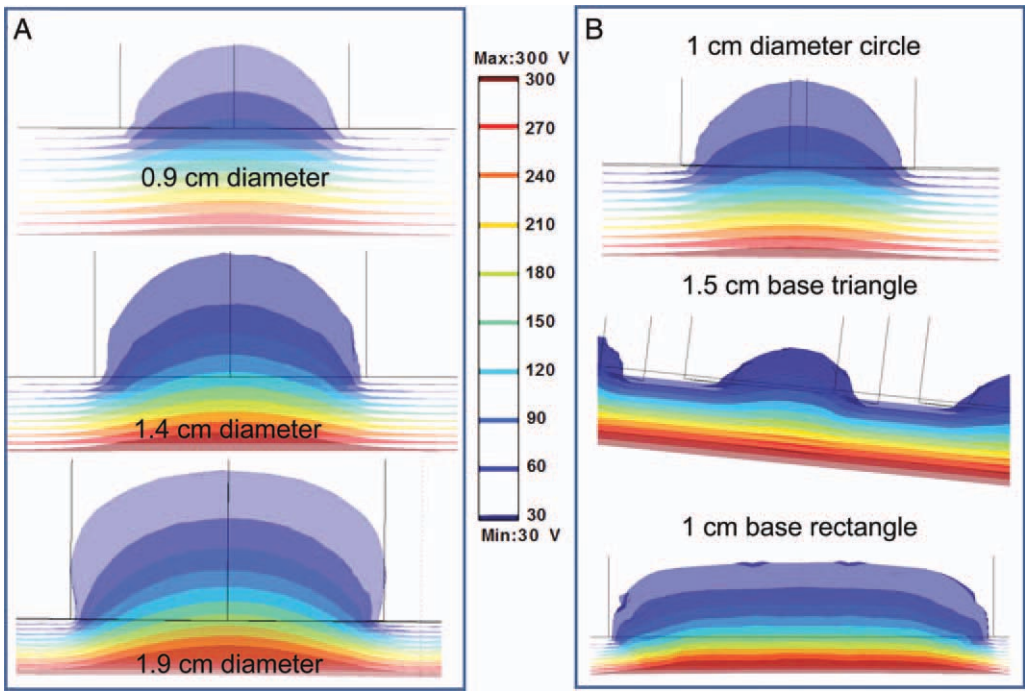

Figure 6. Numerical solution showing the equipotential lines in the electrical field with different void sizes and shapes. (A) Different circular void diameters under 12 kV applied voltage. (B) Different void shapes under 10 kV. [Color figure can be viewed in the online issue, which is available at wileyonlinelibrary.com.]

the aluminum surfaces, and the density of fibers in the air gap is lower than that at aluminum foil; the large pore size of fibers exist in the air gap of the novel collector plate.

We also evaluated the relationship between the electric fields and the size and shape of the voids in the collector plate. Isopotential surfaces and magnified views with different size [Figure 6(A)] and shape of the voids [Figure 6(B)] in the collector plates are shown. With identical color scales, the cup shape of the isopotential surfaces are extended into the void, which indicates that the path length increased between the isopotential surface at the aluminum foil to that inside the void. Therefore, the single fiber is less probable to escape the electrostatic force and enter the voids. When the void size increases, the cup shape of the isopotential surfaces becomes wider and the possibility of fiber depositing in the void becomes low. Thus, the pore size between the fibers increases with the void size.

When the shape of the void was triangular and rectangular [Figure 6(B)], the fibers are aligned due to the dragging force of electric fields. The drag force generated by the electric field is perpendicular to the isopotential surfaces and the polymer fibers at the edge of triangular void to take the shorter paths. Thus, single fibers align at the edge of the triangular void and the width of the rectangular void. The fibers aligned when deposited at the edge of the triangular void in the collector plate. The strong electric forces at the void edges will stretch the polymer fibers and form the aligned scaffold.[20] Such potential distribution pattern prompts the possible ways of optimizing the collector design. As mentioned, the drag force forms along the steepest descent direction, to deposit the polymer fibers at the aluminum foil plane. Optimized design should facilitate further collapse of the isopotential surface in the voids.

DISCUSSION

Electrospinning is a versatile method to fabricate micro and nanofibers from a variety of biomaterials for tissue regeneration and other medical applications. Under the electrical field, the solvent evaporates and the polymer fibers travel to the collector plate where they are deposited as a random nonwoven mat,[21] because the direction of the spraying jet is randomized due to the bending instability of the charged jet.[22] As pore size is an issue for cell infiltration, previously we reported on a novel technique to form fibers with pore sizes sufficient for cell infiltration and colonization. The void in the collector plate allowed the formation of structures with large pore sizes. In this study, we extended the analyses to the effect of void size and shape in the collector plate. Results showed that under the solution and process parameters the fiber diameter was the same and independent of the geometrical patterns of the voids in the collector plates. Two different solvents systems were used with variation in volatility and conductivity. Despite these variations, no significant effect of the void size or shape was observed in the corresponding group. However, one has to compare the effect of different solvents on the fiber morphology to better understand the effect of voids.[23]

First, the pore size increased with the circular void size without affecting the distribution pattern of the fibers. However, distribution pattern changes with shape of the void; the fibers aligned when deposited at the edge of the triangular void and across

the rectangular void. These trends are similar to the fiber patterns in gold/quartz collector plates.[24] When a void is introduced into the quartz collector plate, the insulated area changes the structure of the electric field, resulting in geometrical change of the fiber patterns.[24,25] When a specific shape of the insulated void is introduced into a conductive collector plate, the distribution of the electric field is more complex like the circular void,[24] suggesting the need for understanding the changes in the electric fields. For this purpose, we used COMSOL Multiphysics to understand the changes in the electrical field. Simulations were performed under conditions identical to the experimental setup. These results showed isoelectric regions similar to the alignment of fibers in different void shapes. However, size of the void did not have significant influence in the pattern of isoelectric lines. Thus, one could align fibers by altering the void shape. Because the collector plate can be handled without affecting the fibers, low density of the fibers in the void lead to increased pore size of scaffolds. This could be of significant importance in regenerating tissues using required orientation of fibers.

We also tested the effect of molecular weight of PCL on fiber formation and characteristics.[26] As the molecular weight increases, degradation time increases (PCL10K for 2 month, PCL45K for 6 months, and PCL80K for 2 years).[27,28] We fabricated PCL80K fibers in combination with low molecular weight (PCL45K and PCL10K). We showed that the mixing ratio of polymer solution with different molecular weight does not affect the structure of fibers. The fiber diameter, shape factor, and the pore size of the scaffold were almost the same under the same conditions of process parameters (needle size, flow rate, and distance between the needle tip and the collector plate) with different molecular weights of PCL was changed in a mixture of chloroform and methanol. However, the effect of viscosity changes due to the mixing of different polymers and solvent permittivity on fiber size needs to be evaluated.[29] Formed fibers were further evaluated for degradation under physiological conditions for 30 days. Before the degradation test, the fiber morphologies with different molecular weight were identical. After 30 days, the fibers with low molecular weight PCL showed more damaged area on the surface, suggesting that PCL80K fibers with PCL45K and PCL10K were more degradable than PCL80K fibers. Degradation of PCL consists of two steps:[30] in the first step, water diffuses into the amorphous regions and hydrolyze the ester bonds, reducing the molecular weight of the polymer without affecting the structural weight; in the second step, the amorphous regions degrade, hydrolysis of the crystalline domain occurs leading accelerated weight loss.[31] Weight loss of the structures could not be determined during the degradation time, primarily due to the problems encountered during sample collection and processing to determine dry weight. However, we suspect the degradation to be only the first stage over the 30 days as the entire fibrous structure was stable during the degradation period with partial damage to the fibers.

CONCLUSIONS

In summary, introduction of voids in the collector plate helps in generating structures with large pore sizes suitable for cell infiltration. Increase in void size increases the distance between the fibers, that is, pore sizes. By changing the shape of the collector plate, fibers can be aligned without altering the fiber size and structure at the same processing and solution conditions. Simulations results confirmed that altered alignment of fibers in different shapes is due to the altered electrical field within the void. Results also showed that the fibers can be formed by blending different molecular weight PCL and pattern of degradation can be studied at the individual fiber level. One has to extend these results to other polymer systems and applications.

REFERENCES

1. Hong, J. K.; Madihally, S. V. *Tissue Eng. Part B Rev.* **2011,** *17*, 125.
2. Shang, S.; Yang, F.; Cheng, X.; Walboomers, X. F.; Jansen, J. A. *Eur. Cell Mater.* **2010,** *19*, 180.
3. Choi, J. S.; Lee, S. J.; Christ, G. J.; Atala, A.; Yoo, J. J. *Biomaterials* **2008,** *29*, 2899.
4. Corey, J. M.; Gertz, C. C.; Wang, B. S.; Birrell, L. K.; Johnson, S. L.; Martin, D. C.; Feldman, E. L. *Acta Biomater.* **2008,** *4*, 863.
5. Chew, S. Y.; Mi, R.; Hoke, A.; Leong, K. W. *Biomaterials 29*, 653 **2008.**
6. Zhong, S.; Teo, W. E.; Zhu, X.; Beuerman, R. W.; Ramakrishna, S.; Yung, L. Y. *J. Biomed. Mater. Res. A* **2006,** *79*, 456.
7. Ma, Z.; He, W.; Yong, T.; Ramakrishna, S. *Tissue Eng.* **2005,** *11*, 1149.
8. Courtney, T.; Sacks, M. S.; Stankus, J.; Guan, J.; Wagner, W. R. *Biomaterials* **2006,** *27*, 3631.
9. O'Brien, F. J.; Harley, B. A.; Yannas, I. V.; Gibson, L. *Biomaterials* **2004,** *25*, 1077.
10. Li, D.; Wang, Y. L.; Xia, Y. N. *Adv. Mater.* **2004,** *16*, 361.
11. Park, S. H.; Yang, D. Y. *J. Appl. Polym. Sci.* **2011,** *120*, 1800.
12. Li, D.; Ouyang, G.; McCann, J. T.; Xia, Y. *Nano Lett.* **2005,** *5*, 913.
13. Jha, B. S.; Colello, R. J.; Bowman, J. R.; Sell, S. A.; Lee, K. D.; Bigbee, J. W.; Bowlin, G. L.; Chow, W. N.; Mathern, B. E.; Simpson, D. G. *Acta Biomater.* **2011,** *7*, 203.
14. Hong, J. K.; Madihally, S. V. *Acta Biomater.* **2010,** *6*, 4734.
15. Oh, S. H.; Park, I. K.; Kim, J. M.; Lee, J. H. *Biomaterials* **2007,** *28*, 1664.
16. Zhang, Y.; Deng, X.; Scheller, E. L.; Kwon, T.-G.; Lahann, J.; Franceschi, R. T.; Krebsbach, P. H. *Biomaterials* **2010,** *31*, 3231.
17. Munir, M. M.; Suryamas, A. B.; Iskandar, F.; Okuyama, K. *Polymer* **2009,** *50*, 4935.
18. Koski, A.; Yim, K.; Shivkumar, S. *Mater. Lett.* **2004,** *58*, 493.
19. Mondalek, F. G.; Lawrence, B. J.; Kropp, B. P.; Grady, B. P.; Fung, K. M.; Madihally, S. V.; Lin, H. K. *Biomaterials* **2008,** *29*, 1159.

20. Li, D.; Wang, Y. L.; Xia, Y. N. *Nano Lett.* **2003,** *3*, 1167.

21. Li, D.; Wang, Y.; Xia, Y. *Adv. Mater.* **2004,** *16*, 361.

22. Reneker, D. H.; Yarin A. L.; Fong, H.; Koombhongse, S. *J. Appl. Phys.* **2000,** *87*, 9.

23. Wannatong, L.; Sirivat, A.; Supaphol, P. *Polym. Int.* **2004,** *53*, 1851.

24. Li, D.; Ouyang, G.; McCann, J. T.; Xia, Y. *Nano Lett.* **2005,** *5*, 913.

25. Li, D.; Wang, Y.; Xia, Y., *Nano Lett.* **2003,** *3*, 1167.

26. Cottam, E.; Hukins, D. W. L.; Lee, K.; Hewitt, C.; Jenkins, M. *J. Med. Eng. Phys.* **2009,** *31*, 221.

27. Chan-Chan, L. H.; Solis-Correa, R.; Vargas-Coronado, R. F.; Cervantes-Uc, J. M.; Cauich-Rodríguez, J. V.; Quintana, P.; Bartolo-Pérez, P. *Acta Biomater.* **2010,** *6*, 2035.

28. Lam, C. X. F.; Savalani, M. M.; Teoh, S.-H.; Hutmacher, D. W. *Biomed. Mater.* **2008,** *3*, 034108.

29. Guarino, V.; Cirillo, V.; Taddei, P.; Alvarez-Perez, M. A.; Ambrosio, L. *Macromol. Biosci* **2011,** *11*, 1694.

30. Hartman, O.; Zhang, C.; Adams, E. L.; Farach-Carson, M. C.; Petrelli, N. J.; Chase, B. D.; Rabolt, J. F. *Biomaterials* **2010,** *31*, 5700.

31. Jones, D. S.; Djokic, J.; McCoy, C. P.; Gorman, S. P. *Biomaterials* **2002,** *23*, 4449.